Journal of Electroceramics, 13, 703–706, 2004

Development of Resistive Oxygen Sensors Based on Cerium Oxide Thick Film

NORIYA IZU,* WOOSUCK SHIN, ICHIRO MATSUBARA & NORIMITSU MURAYAMA

Synergy Materials Research Center, National Institute of Advanced Industrial Science and Technology, Moriyama-ku, Nagoya 463-8560, Japan

Submitted March 7, 2003; Revised March 3, 2004; Accepted March 4, 2004

Abstract. It is important to shorten the response time of resistive oxygen sensor in order to reduce harmful emission of automobiles. The diffusion and surface reaction theory tells us that reducing particle size leads to shortening the response time. The fine ceria powder was prepared a by new precipitation method and the oxygen sensors having ceria thick film with the particle size of 120 nm were fabricated using fine ceria (cerium oxide) powder. The thick film exhibited good adhesion to alumina substrate. The value of n in $R \propto P(O_2)^{1/n}$ at 1073 and 1173 K were 6.2 and 6.4 in the oxygen partial pressures range from 10^{-13} to 10^5 Pa, respectively. The response time for the sensor was 22 and 12 ms at 1073 and 1173 K, respectively. The sensor fabricated in this study showed fast response.

Keywords: oxygen gas sensor, ceria, fast response, precipitation method, carbon powder

1. Introduction

Oxygen gas sensors have come into wide use as automotive exhaust gas sensors of gasoline-powered vehicles [1]. In addition it is expected that they will be applied to diesel engines and two-wheeled vehicles. Further a second oxygen sensor is required downstream of the catalysts to monitor all emission components (On Board Diagnosis –OBD) [2]. Therefore, the market of oxygen gas sensors will continue to grow in future.

Recently, resistive-type oxygen gas sensors [3–8] are drawing the attention again for such new applications since their structure is simpler and their size is smaller compared to conventional oxygen gas sensors using concentration cells consisting of oxygen-ion-conductor [7, 8]. The oxygen gas sensors for automotive exhaust gas need not only small size but also fast response in order to monitor the concentration of oxygen for controlling the air to fuel ratio completely. In order to improve the response of the sensors, Beie and Gnörich [7] investigated the oxygen gas sensing properties of thick films of cerium oxide (ceria), which exhibits a high diffusion coefficient for oxygen vacancy. In their work, thick films were formed by screen printing with the paste including cerium oxide powders with an average particle size of micron order. The response time of those sensors was in the range of minutes. Very recently, we synthesized the fine ceria powder by mist pyrolysis and fabricated the oxygen sensors having ceria thick film with the particle size of 200 nm from the powder [9]. Those sensors showed faster response compared to that with the particle size of micron order.

The new precipitation method using carbon powder [10, 11] has been developed as the synthesis method for fine powder with particle size of less than 500 nm. This new precipitation method makes larger synthesis quantity of the powder than mist pyrolysis method. So in this study we synthesized the fine ceria powder by the new precipitation method and fabricated the oxygen sensors having ceria thick film with the particle size less than 200 nm. The sensor outputs were investigated in the oxygen partial pressures range from 10^{-13} to 10^5 Pa and the fast response of the sensors was measured in the oxygen partial pressure of 20–60 kPa.

*To whom all correspondence should be addressed. E-mail: n-izu@aist.go.jp

2. Experimental

2.1. Preparation of Sensors

The $Ce(NO_3)_3 \cdot xH_2O$ was dissolved in distilled water and stirred for several minutes. The solution was mixed with aqueous ammonia. Then the resulting precipitate was filtrated to obtain the white gel. The white gel was mixed with commercialized carbon powder using hybrid mixer. The mixture was dried at 343 K in air for several hours. The dried mixture was calcined at 1173 K to obtain the fine ceria powder.

The paste was prepared by mixing the fine ceria powder with an organic binder. The organic binder included terpineol and ethyl cellulose. The paste was screen-printed on interdigital structure Pt electrodes with Al_2O_3 substrates. The screen printed thick films were calcined at 773 K for 5 h in air. Then the calcined thick films were fired at 1373 K. The thick films had dimensions of 7 mm $\times$ 7 mm and thickness of 10 μm.

2.2. Characterization of Thick Films and Evaluation of the Output in Wide Oxygen Partial Pressure Range

The thick films were characterized by X-ray diffraction, (XRD: Cu K_α radiation) (RINT2100V/PC, Rigaku Corporation) and scanning electron microscopy, (SEM: JSM-6335F, JEOL).

The resistance of thick film was measured in a tubular furnace in oxygen partial pressure of 10^{-13} to 10^5 Pa at 1073 and 1173 K. The oxygen partial pressure was adjusted with N_2-O_2 or H_2O-H_2 mixtures and measured using a zirconia probe.

2.3. Evaluation of Fast Response

The oxygen partial pressure was suddenly changed from 2×10^4 to 6×10^4 Pa or from 6×10^4 to 2×10^4 Pa by square wave modulation of total pressure for air. Sensor output and oxygen partial pressure, (calculated from total pressure) were measured as a function of time. We defined $t_{90,s}$ and $t_{90,g}$ as the times until sensor output and oxygen partial pressure changed 90% after a sudden change of oxygen partial pressure, respectively.

3. Results and Discussion

The ceria powder obtained by the new precipitation method was investigated by XRD and SEM. The XRD pattern for the ceria powder showed one phase of fluorite structure. The crystallite size calculated from the full width as half maximum (FWHM) of the peaks was about 40 nm. From the SEM observation, the grain size of the powder was about 50 nm. Therefore, the grain observed by SEM may be one crystallite.

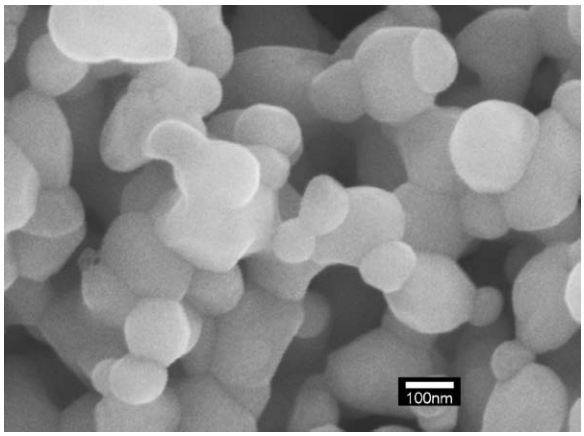

Fig. 1. Microstructure of ceria thick film after firing at 1373 K.

The ceria thick film after firing at 1373 K was also investigated by XRD and SEM. The XRD pattern for the ceria thick film also showed one phase of fluorite structure. The FWHM of the thick film was smaller than that of the powder. The crystallite size calculated from FWHM was about 80 nm. Thus the crystallite size of the thick film was larger than that of the powder. The microstructure observed using SEM is shown in Fig. 1. The thick film had a porous structure and an average particle size of thick film was 120 nm. The particle observed by SEM may include a few crystallites. A SEM photograph of low magnification showed the thick film had no crack. By the peeling test using commercial cellophane tape, it was confirmed that the thick film exhibited good adhesion to alumina substrate.

The relations between oxygen partial pressure ($P(O_2)$) and the resistance (R) as sensor output at 1073 and 1173 K are shown in Fig. 2. The value of n in $R \propto P(O_2)^{1/n}$ at 1073 and 1173 K were 6.2 and 6.4. The mechanism of electrical conductivity for ceria has been reported [12, 13].

$$2Ce_{Ce}^{X} + O_O^X = 2Ce'_{Ce} + V_O^{\cdot\cdot} + 1/2O_2 \qquad (1)$$

where Ce_{Ce}^{X} and O_O^X represent the regular lattice ions while Ce'_{Ce} and $V_O^{\cdot\cdot}$ are the charged defects. Ce'_{Ce} and $V_O^{\cdot\cdot}$ show the electron trapped by $Ce_{Ce}{}^{X}$ and double

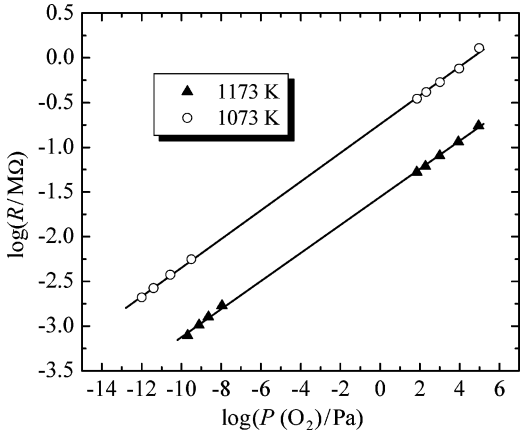

Fig. 2. The relations between oxygen partial pressure ($P(O_2)$) and the resistance (R) as sensor output at 1073 and 1173 K: (○) at 1073 K, and (▲) at 1173 K.

ionized oxygen vacancy, respectively. The electrons are assumed localized in CeO_{2-x} since the electron conduction process is a "hopping type" process [12, 14]. Eq. (1) can be expressed as

$$K = [Ce_{Ce}{}']^2[V_O^{\cdot\cdot}]P(O_2)^{1/2} \tag{2}$$

where K is the equilibrium constant of the Eq. (1), $[Ce'_{Ce}]$ and $[V_O^{\cdot\cdot}]$ are the concentration of Ce'_{Ce} and $V_O{}^{\cdot\cdot}$, respectively. Electrical neutrality holds as follows.

$$[Ce'_{Ce}] = 2[V_O^{\cdot\cdot}] \tag{3}$$

Therefore, the next relation is derived from Eqs. (2) and (3).

$$[Ce'_{Ce}] = 2[V_O^{\cdot\cdot}] \propto P(O_2)^{-1/6} \tag{4}$$

The total electrical conductivity σ is the following relation:

$$\sigma = [Ce'_{Ce}]e\mu_e \tag{5}$$

where μ_e is the mobility of electron and ion conductivity is negligible. Therefore, the next relation is derived from Eqs. (4) and (5).

$$R \propto 1/\sigma \propto P(O_2)^{1/6} \tag{6}$$

This equation means the value of R is proportional to $P(O_2)^{1/6}$. From our result that the value of n was approximately 6, it was considered that the oxygen sensor fabricated in this study obeyed the mechanism described above.

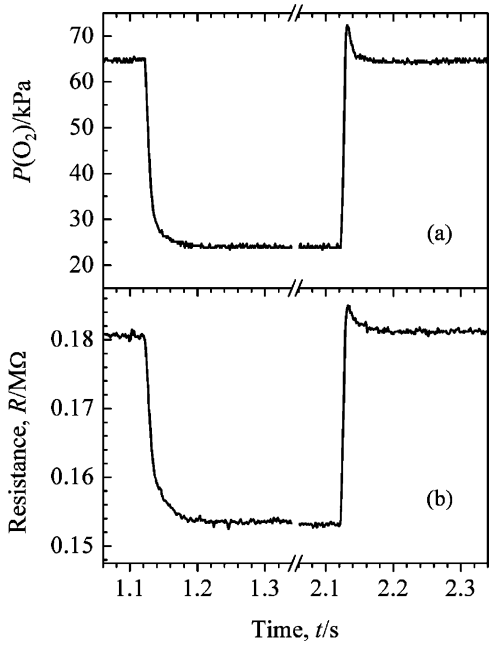

Fig. 3. The typical sensor output change in the case of the sudden change of oxygen partial pressure from 65 to 25 kPa or from 25 to 65 kPa: (a) oxygen partial pressure change, and (b) sensor output change at 1173 K.

It has been reported that the relation between log of R and log of $P(O_2)$ has no linear relation at the range of high oxygen partial pressure in the case of the resistive oxygen sensor based on titania [3]. So it is used only for the sensor detecting the stoichiometric ratio of air to fuel, but is not used for the sensor detecting air to fuel ratio of lean-burn engine. On the contrary, since the resistive oxygen sensor based on ceria can measure oxygen partial pressure in the wide range of air to fuel ratio, it can be used for not only the sensor detecting the stoichiometric ratio of air to fuel but also the sensor detecting air to fuel ratio of lean-burn engine.

Next, the fast response time for the oxygen sensor in high oxygen partial pressure was investigated. Figure 3 shows the typical sensor output change in the case of the sudden change of oxygen partial pressure from 65 to 25 kPa or from 25 to 65 kPa. Figure 3(a) shows the change of oxygen partial pressure and Fig. 3(b) shows the change of sensor output at 1173 K. As can be seen in Fig. 3, the response of the oxygen sensor was very fast. The values of $t_{90,s}$ and $t_{90,g}$ show the response

Table 1. Response time for the oxygen sensors based on ceria thick film.

Temperature (K)	Oxygen partial pressure change from high to low			Oxygen partial pressure change from low to high		
	$t_{90,s}$ (ms)	$t_{90,g}$ (ms)	t_{90} (ms)	$t_{90,s}$ (ms)	$t_{90,g}$ (ms)	t_{90} (ms)
1073	42	20	22	9	9	<1
1173	33	21	12	8	8	<1

The values of $t_{90,s}$ and $t_{90,g}$ show the response time for sensor output and oxygen partial pressure, respectively. A corrected response time, t_{90}, was defined as $t_{90,s} - t_{90,g}$.

time for sensor output and oxygen partial pressure, respectively. The values of $t_{90,s}$ in the case of the oxygen partial pressure change from high to low and the value of $t_{90,g}$ in the case of the change from low to high are summarized in Table 1. Since the value of $t_{90,s}$ include the time required for the oxygen partial pressure change, i.e., $t_{90,g}$, the precise response time of the oxygen sensor is smaller than $t_{90,s}$. A corrected response time, t_{90} was defined as $t_{90,s} - t_{90,g}$ and is summarized in Table 1. When oxygen partial pressure changed from low to high, the response of the oxygen sensor was very fast. When $t_{90,s} - t_{90,g}$ was simply calculated for the change from low to high, it was 0. However, when the measurement accuracy was taken into consideration, t_{90} was less than 1 ms or less. On the other hand, in the case of the oxygen partial pressure change from high to low, t_{90} was approximately 22 and 12 ms at 1073 and 1173 K, respectively. It became clear that the response time of oxygen sensor for the oxygen partial pressure change from high to low was slower compared to the response time for the change from low to high. From this result, it seemed that the response mechanism was different between the oxygen partial pressure change from high to low and the change from low to high. It was reported the response time of the oxygen sensor based on ceria was 100 ms at 1073 K [15]. The sensor fabricated in this study showed fast response. It was confirmed that reducing the particle size resulted in shortening response time.

4. Conclusion

We prepared the fine ceria powder by the new precipitation method and fabricated the oxygen sensors having ceria thick film with the particle size of 120 nm. The thick film exhibited good adhesion to alumina substrate. The value of n in $R \propto P(O_2)^{1/n}$ at 1073 and 1173 K were 6.2 and 6.4 in the oxygen partial pressures range from 10^{-13} to 10^5 Pa, respectively. The response time for the sensor was 22 and 12 ms at 1073 and 1173 K, respectively. It was confirmed that reducing the particle size resulted in shortening response time.

References

1. M. Ogita, K. Higo, Y. Nakanishi, and Y. Hatanaka, *Applied Surface Science*, **175/176**, 721 (2001).
2. J. Riegel, H. Neumann, and H.-M. Wiedenmann, *Solid State Ionics*, **152/153**, 783 (2002).
3. M.J. Esper, E.M. Logothetis, and J.C. Chu, SAE, paper 790140 (1979).
4. A. Takami, T. Matsuura, T. Sekiya, T. Okawa, and Y. Watanabe, SAE, paper 850381 (1985).
5. U. Lampe, J. Gerblinger, and H. Meixner, *Sensors and Actuators B*, **7**, 787 (1992).
6. D. Pribat and G. Velasco, *Sensors and Actuators*, **13**, 173 (1988).
7. H.-J. Beie and A. Gnörich, *Sensors and Actuators B*, **4**, 393 (1991).
8. J. Sheng, N. Yoshida, J. Karasawa, and T. Fukami, *Sensors and Actuators B*, **41**, 131 (1997).
9. N. Izu, W. Shin, N. Murayama, and S. Kanzaki, *Sensors and Actuators B*, **87**, 95 (2002).
10. N. Murayama, W. Shin, N. Izu, M. Hayashi, and S. Sago, in *Proceedings of the 5th East Asian Conference on Chemical Sensors* Nagasaki, Japan (2001), p. 243.
11. N. Murayama, W. Shin, S. Sago, and M. Hayashi, Published Patent Application of Japan, 2002-255515, in Japanese.
12. R.J. Panlener, R.N. Blumenthal, and J.E. Garnier, *J. Phys. Chem. Solids*, **36**, 1213 (1975).
13. N. Izu, W. Shin, and N. Murayama, *Sensors and Actuators B*, **87**, 99 (2002).
14. H.L. Tuller and A.S. Nowick, *J. Phys. Chem. Solids*, **38**, 859 (1977).
15. E. Ivers-Tiffée, K. H. Härdtl, W. Menesklou, and J. Riegel, *Electrochimica Acta*, **47**, 807 (2001).